

Competitive Adhesion Reduces the Effective Bridging Length of Polymers

Lars Sonnenberg,^{*,†} Laurent Billon,[‡] and Hermann E. Gaub[†]

Lehrstuhl für Angewandte Physik and Center for NanoScience, Ludwig-Maximilians-Universität München, Amalienstr. 54, 80799 München, Germany, and IPREM/EPCP UMR 5254, Université de Pau et des pays de l'Adour, Hélioparc Pau-Pyrénées, 2 Av Président Angot, 64053 Pau Cedex 09, France

Received November 22, 2007; Revised Manuscript Received February 18, 2008

ABSTRACT: Surface end-grafted poly(acrylic acid) (PAA) chains were investigated by AFM-based single molecule force spectroscopy. Upon adsorption on the surface of the AFM tip, the molecules bridge the two surfaces. By retracting the tip from the sample, the molecules were desorbed from the tip surface and the bridging lengths were measured. The comparison of the observed bridging length distribution with the molecular length distribution as obtained by GPC revealed that tip and sample surface compete for the polymer. In the case of higher adsorption strength to the tip surface the polymer chains bridge with their entire lengths while in the opposite case the polymers try to maximize the surface coverage. In the latter, the bridging lengths are reduced depending on the grafting density of the polymer monolayer.

Introduction

Material properties of modern particle–polymer composites crucially depend on adhesion of the polymers to the particle surfaces and as a result on the effective bridging properties of the polymers.^{1,2} The interaction of polymers with interfaces is quite generally of utmost technological importance but also comprises a richness of fundamental science phenomena.^{3,4} Particularly polyelectrolyte and hydrated surfaces have gained attention not only because of their applications, e.g. in solvent-free coatings, but also because of their model character for a richness of questions in life sciences ranging from surface fouling to biopolymer adhesion in tissue replacements.

In dispersions polyelectrolytes are employed to stabilize colloidal particles in solution via steric and/or electrostatic repulsion.^{5–7} They may also clot particles together, i.e. filter unwanted particles out, via polymer bridges.^{8–10} Such polymers are frequently end-grafted to the particle surface to enhance long-term stability and to prevent the polymer from desorbing at low interaction strength.^{11–14} Particularly interesting properties with many applications in smart materials may be achieved when the interaction/bridging properties can be tuned by external stimuli. Using polyelectrolytes (PELs) for such purposes allows the manipulation of electrostatic interactions by varying the salt concentration and/or pH of the aqueous solution.^{3,4,15}

In this study we investigated the bridging of individual PEL chains between two surfaces^{16,17} by means of AFM force spectroscopy.^{18–21} On one end the polymers were grafted to a planar silicon oxide surface. As counter-surface we approached the polymer with the blunt tip of an AFM cantilever (see Figure 1) and allowed it to adsorb onto this tip. As a result, the tip was pulled toward the silicon oxide surface. When retracting the AFM tip, the PEL chains successively desorbed from the tip surface, and at the same time the interaction forces were measured with piconewton precision and the bridging lengths with nanometer accuracy at the level of single molecules.

In a previous paper we showed that AFM desorption measurements allow for the investigation of PEL monolayers and observed that the bridging lengths are a function of the pH

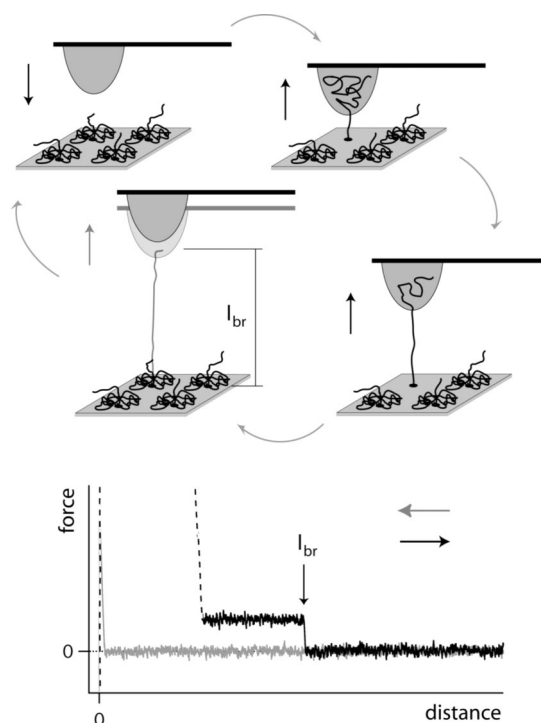


Figure 1. A single molecule desorption experiment with surface-grafted polymers by means of an AFM. When approaching the AFM tip to the surface, polymer chains adsorb on the tip surface. Upon retracting the AFM tip, the polymer successively desorbs from the tip. As in our case here, the interaction dynamics of the adsorbed polymer is much faster than the retraction velocity of the AFM tip; the desorption process occurs under equilibrium conditions. This results in a constant speed-independent adhesion force, which equals the change in Gibbs free energy per unit length of the polymer.^{24–31} Upon further retracting the tip, the plateau force finally drops to zero when the polymer chain detaches completely from the tip. The corresponding distance is named the bridging length l_{br} . If the grafting density is high and several polymers adhere to the tip, they may detach one after the other upon withdrawing the tip, resulting in a staircase-like pattern of the force–distance records (see also Figure 2).

of the aqueous solution when using silicon nitride AFM tips.²² Since the interaction force of the poly(acrylic acid) chains and the tip surface also depends on the pH, we proposed a model

* Corresponding author. E-mail: sonnenberg@physik.uni-muenchen.de.

[†] Ludwig-Maximilians-Universität München.

[‡] Université de Pau et des pays de l'Adour.

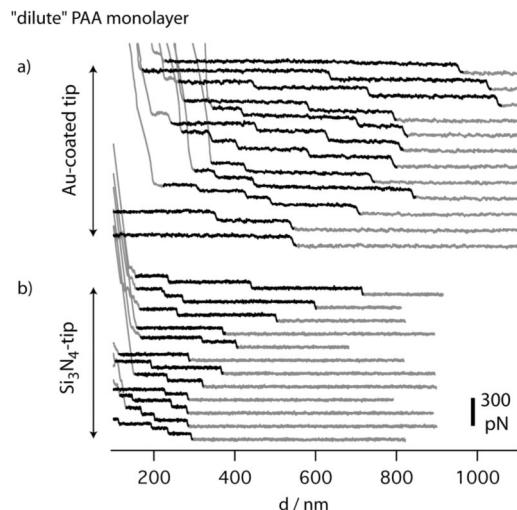


Figure 2. Force–distance curves measured at randomly chosen positions on a poly(acrylic acid) (PAA) monolayer grafted at a density of $1/460 \text{ nm}^{-2}$ (“dilute” monolayer) with a gold-coated tip (a) and a silicon nitride tip (b). Both measurement series were conducted in an aqueous solution containing 100 mM NaCl at pH 6.

to explain the correlation between desorption force and apparent bridging length.²³ The model of differential polymer adhesion takes into account two different processes: the continuous desorption of the polymer from the surface and the instantaneous complete detachment of the adherent polymer chain from the surface. It was possible to explain the reduction of the measured bridging length at alkaline pH in comparison to the length of the initially adsorbed polymer segment as observed at low to neutral pH values. However, the latter may be considerably smaller than the contour length of the corresponding PEL chain. In this paper we therefore aim to study the correlation of the distribution of adsorbed polymer lengths with the molecular length distribution of the PEL monolayer as obtained with gel permeation chromatography (GPC).

By modification of the surface chemistry of the tip or by metal evaporation, we altered the interaction with the polymer and explored the vertical structure of the adsorbate film. The minuteness of the tip and its curvature radius below 100 nm furthermore make it an excellent model system for a nanoparticle and its polymer interaction in a nanocomposite material.

Materials and Methods

Monolayers of covalently end-grafted poly(acrylic acid) (PAA) ($-\text{CH}_2\text{CHCOOH}-$)_n chains were synthesized with the grafting-from technique under controlled/living radical polymerization conditions. Afterward, the samples were characterized with gel permeation chromatography (GPC) and X-ray photoelectron spectroscopy (XPS) in order to determine the molecular weight distribution of the polymers and the grafting density on the surface.

GPC characterization was performed using a 2690 Waters Alliance System with THF as the eluent. It was equipped with four Styragel columns HR 0.5, 2, 4, and 6 working in series at 40 °C, a 2410 Waters refractive index detector, a 996 Waters photodiode array detector, and a Wyatt light scattering multiangle detector. A calibration curve established with low-polydispersity polystyrene (PS) standards was used for the determination of the molecular weights. The molecular weight distribution of the free polymer chains was characterized with GPC in THF after methylation of PAA to poly(methyl acrylate), yielding an organo-soluble polymer—a procedure commonly accepted to avoid specific polymer–polymer or polymer–substrate interactions present in the aqueous phase.³² Because of the absolute molecular weight of the polyacrylate in THF at 40 °C as determined by light scattering being close to that of the PS standard, $\log(M_{\text{abs}}) = 0.9849 \log(M_{\text{PS}})$, the molecular

weight distribution of PAA is directly extracted from PS data. For further details concerning synthesis and characterization see refs 22, 32, and 33.

The investigated samples are for differentiation named “dense” and “dilute”; their grafting densities were estimated as $\sigma_{\text{dense}} \approx 1/200 \text{ nm}^{-2} \approx 2.3\sigma_{\text{dilute}}$.

All force spectroscopy experiments were conducted on a home-built instrument using silicon nitride cantilevers (Microlever) purchased from Veeco Instruments. For some experiments the cantilevers were in addition thermally coated with a few nanometers of CrNi followed by a 40 nm thick gold layer. Single molecule desorption experiments were conducted to measure the bridging length l_{br} of the PAA chains between the sample surface *S* and the AFM tip *A* as well as the adhesion force F_{A} of the PAA molecules to the AFM tip with high precision.

As illustrated in Figure 1, the bridging length is defined as the distance at which the polymer chain detaches completely from the AFM tip and the desorption force drops to zero. The measured bridging lengths were found to be independent of the contact time of AFM tip and PAA monolayer. In those desorption experiments the adsorption of the molecules on the AFM tip is completely reversible; that is, the AFM tip does not become contaminated with polymer during the experiments as was tested after the experiments by looking at the interaction between the used AFM tip and a bare silica surface.

Details concerning this technique applied to surface grafted polymers are given in Figure 1 and in refs 22 and 23. Histograms of the obtained bridging lengths were then compared to the corresponding GPC length distributions.^{22,34,35}

In AFM experiments on grafted polymers two types of force–distance curves can be obtained during retraction depending on the chosen polymer, adsorbing surface, and experimental conditions. First, the continuous desorption of the polymer from the surface leading to plateaus of constant force as reported here and second the elastic stretching of the bridging segment which results in a Langevin-like force–extension curve. Besides the polymer–surface adsorption force, the lateral mobility of the polymer on the surface determines which behavior is observed in the experiment.^{36,37}

If the polymer’s lateral mobility on the surface is high compared to the retraction velocity of the AFM tip, the polymer is able to rearrange on the surface, and as a consequence the desorption process takes place under equilibrium conditions. If so, the polymer chain is continuously pulled off from the surface, and a desorption plateau is obtained in the force–extension spectra. Note that desorption plateaus are observed for Gibbs free energies per unit length of tens of $k_{\text{B}}T$ and are therefore not restricted to low adsorption forces. However, the solvent quality for the polymer seems to play a role in this context.^{22,38,39}

For a low lateral mobility the polymer is pinned to the adsorbing surface on the time scale of the experiment, and the force–extension curves show the elastic stretching of the bridging polymer segment. In the case of multiple pinning points, i.e., a polymer that forms loops on the surface, the loop-size distribution can be measured and from the loop lengths of a single molecule the entire length of the initially adsorbed segment may be composed.^{17,40} The latter may appear shorter than the contour length because of a nonadsorbed free end of the polymer chain and/or the location of the pinning point on the curved AFM tip.

Whatever the lateral mobility on the adsorbing surface looks like, it should not affect the adsorption process in the beginning of the experiment when the AFM tip is in contact with the polymer monolayer. The results presented in this paper for the length of the adsorbed polymer segment in comparison to the contour length of the polymer chain should therefore be universally valid and independent of what kind of unbinding behavior is observed later on.

Results and Discussion

In several studies with different polymers we found in the past that the measured bridging lengths depend on both the

properties of the surfaces and the ambient conditions.^{41,42} Hence, we investigated this phenomenon on a well-defined sample with end-grafted PELs.^{22,23,33} Figure 2 shows several representative force–distance curves from desorption measurements performed on a poly(acrylic acid) (PAA) monolayer. In Figure 2a a gold-coated AFM tip and in Figure 2b a bare silicon nitride tip were used. The average numbers of plateaus, i.e., the number of adhered polymers, were found to be comparable, but the desorption force for the PAA chains from the gold-coated tip (95 ± 2 pN) clearly exceeded the desorption force from the silicon nitride tip (65 ± 2 pN). In addition, the observed bridging lengths were found to be correlated with the desorption force; i.e., longer plateaus were found in the case of the gold-coated AFM tip.

This finding clearly shows that the tip surface and the sample surface compete for the polymer: in the case where the adhesion to the tip is stronger than to the sample ($F_A > F_S$), the entire polymer chain will adsorb onto the AFM tip as soon as the contact is formed because the adsorption enthalpy is maximized. This is what we find when we compare the distribution of the measured bridging length as observed with the gold-coated tip with the length distribution of the polymers determined by gel permeation chromatography (GPC distribution) (see Figure 3a). The excellent agreement between the bridging length measured by AFM and the contour length determined by GPC nicely demonstrates that in this regime the AFM-based technique obviously is well suited to measure the length distribution of the grafted polymers with superb precision, sensitivity, and lateral resolution at a moderate experimental effort. However, these experiments also suggest that a much more detailed picture on the internal organization of the grafted polymer layer may be obtained if the adhesion between tip and polymer is gradually reduced. If the adhesion of the polymers to the sample surface is higher than to the tip ($F_A < F_S$), the polymer will maximize its coverage on the sample surface. At the given adhesion enthalpies of $10\text{--}20 k_B T/\text{Kuhn length}$ this will result in a predominantly 2d conformation as was recently shown.⁴³ However, if the coverage exceeds a monolayer, no free surface is left, and the remaining segments of the polymer are dangling off the surface or, if the solvent is poor (which is not the case in our experiments here), they may interact with the adsorbed monolayer. If such a surface is probed with an AFM tip, only the dangling section of the polymer will adhere to the tip, and as a consequence only this section will bridge the gap between the two surfaces upon separation. This is what we find when we probe the same sample as in Figure 3a (“dilute” PAA monolayer) with a bare silicon nitride tip (see Figure 3b). The histogram of the bridging lengths is clearly shifted toward shorter lengths.

If the model discussed above holds true, an increase in grafting density should reduce the free area on the sample surface and as a result should lengthen the dangling section of the grafted polymers. This was tested with a “dense” PAA monolayer, which had a grafting density of $\sigma_{\text{dense}} = 1/200 \text{ nm}^{-2}$. An identical experiment as the one described above resulted in the bridging length histogram in Figure 3c, which does not fully reproduce the GPC distribution but shows significantly longer bridging lengths than those measured on the “dilute” sample. Again, already this qualitative result demonstrates that valuable information on the vertical structure of the grafted layer may be obtained with this single molecule approach.

A quantitative description of these effects will be developed in the following. The case $F_A > F_S$ needs no quantitative model: upon contact, the entire length of the polymer is “sucked” onto the tip and the polymer bridges with its full length. In the case $F_A < F_S$ only that section of the polymer adheres to the tip, which is not adsorbed to the sample surface. Would the lateral mobility of the polymer at the sample surface be high, adjacent

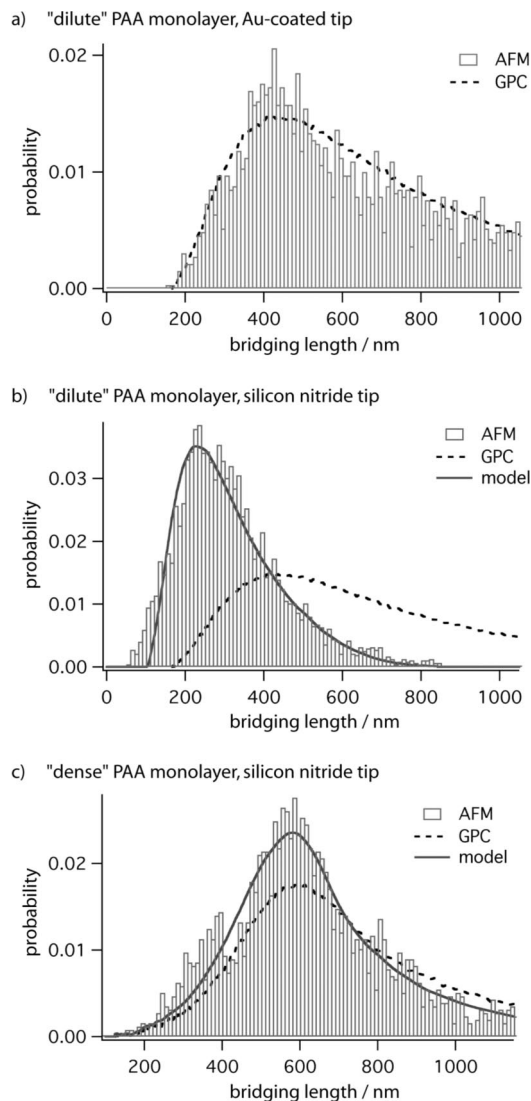


Figure 3. Distribution of bridging lengths determined by AFM desorption measurements in comparison with the molecular length distributions obtained by GPC: (a) “dilute” PAA monolayer investigated with gold-coated AFM tip, (b) “dilute” PAA monolayer with Si_3N_4 tip, and (c) “dense” PAA monolayer with Si_3N_4 tip. Moreover, the AFM results of (b) and (c) were fitted with the described model: $b = 1.5 \text{ nm}$ and $\nu = 0.588$ (b) and $\nu = 0.553$ (c). All measurements were conducted in an aqueous solution containing 100 mM NaCl at pH 6.

polymers would compete for the bare surface and neighboring polymers would creep into voids caused by fluctuations. In this case the polymer would be displaced at the surface and would adsorb on the AFM tip with its entire length. From the findings in Figure 3 we would therefore conclude a low lateral mobility of the polymers on the sample surface. In the case of the “dilute” monolayer the average distance between the grafting points matches the end-to-end distance of the polymer in 3d. By this way, each polymer may in the average occupy its projection area on the sample surface. On the basis of the Rouse–Zimm model for polymers, the area which each polymer may adhere to is therefore on the order of $A = \pi(R/2)^2$ with $R = a^{1-\nu}l_c^\nu$. Therein, a is the monomer length (0.25 nm for PAA), l_c the contour length, and $\nu = 0.588$ the critical exponent for a polymer in 3d.⁴⁴ The length of the surface adherent section of the polymer is then given by $l_s = A/b$, where b is the effective width of the polymer. In a densely packed monolayer this number will be equal to the diameter of the polymer and any void in the packing will increase its value, whereas loops will decrease it again. If we take the GPC distribution and the calculated l_s as described

above, we have to assume a value of $b = 1.5$ nm in order to obtain the bridging length distribution drawn in Figure 3b (solid line). With these values we find an excellent agreement between the measured bridging length and our calculated distribution.

Whereas in the “dilute” monolayer the area per polymer was 460 nm^2 , it dropped in the “dense” monolayer to 200 nm^2 as determined by XPS. On average each polymer had therefore in the “dense” monolayer an area of $\Delta A \approx 260 \text{ nm}^2$ less available to adsorb to than in the “dilute” sample. The length of the adsorbed polymer section in the “dense” monolayer is thus given by $l_s = (A - \Delta A)/b$. For the calculation of the resulting bridging length distribution (solid line in Figure 3c) the same value for the effective polymer width $b = 1.5$ nm was taken as in the “dilute” sample. However, the critical exponent has to be smaller as the area covered by the polymers must not exceed the area per polymer defined by the grafting density. The best fit was obtained for $\nu = 0.553$. This might be interpreted as a hint that the conformation of the polymer in the “dense” monolayer is deviating from the ideal Gaussian distribution toward an elongated one. But again, the agreement between the calculated and the measured bridging length distribution is remarkable.

Conclusions

Polymers between particles are the essence of modern composite materials given them both strength and ductility in an unprecedented manner. We investigated formation and dynamics as well as stability of such polymer bridges by replacing the particle by the tip of an AFM cantilever. This allowed us to manipulate and at the same time quantify the interaction with the polymer at the level of individual molecules. We discovered that the competition of two unequal surfaces for the interaction with the polymer gives rise to a new set of phenomena including dynamic unbinding and density-dependent bridging lengths. Any attempt to further optimize future composite materials will have to take these competitive aspects into account.

Acknowledgment. We thank J. Parvole for the chemical characterization. Helpful discussions with M. Seitz, S. Kufer, and F. Kühner are gratefully acknowledged. This work was supported by the Deutsche Forschungsgemeinschaft and the Fonds der chemischen Industrie.

References and Notes

- (1) Napper, D. *Polymeric Stabilization of Colloidal Dispersion*; Academic Press: New York, 1983.
- (2) Fendler, J. H. *Chem. Mater.* **1996**, *8*, 1616–1624.
- (3) Netz, R. R.; Andelman, D. *Phys. Rep.* **2003**, *380*, 1–95.
- (4) Dobrynin, A. V.; Rubinstein, M. *Prog. Polym. Sci.* **2005**, *30*, 1049–1118.
- (5) Joanny, J. F.; Leibler, L.; Gennes, P.-G. d. *J. Polym. Sci., Part B* **1979**, *17*, 1073–1084.
- (6) Fritz, G.; Schädler, V.; Willenbacher, N.; Wagner, N. J. *Langmuir* **2002**, *18*, 6381–6390.
- (7) Walker, H. W.; Grant, S. B. *J. Colloid Interface Sci.* **1996**, *179*, 552–560.
- (8) Lafuma, F.; Wong, K.; Cabane, B. *J. Colloid Interface Sci.* **1991**, *143*, 9–21.
- (9) Dickinson, E.; Eriksson, L. *Adv. Colloid Interface Sci.* **1991**, *34*, 1–29.
- (10) Swenson, J.; Smalley, M. V.; Hatharasinghe, H. L. M. *Phys. Rev. Lett.* **1998**, *81*, 5840–5843.
- (11) Milner, S. T. *Science* **1991**, *251*, 905–914.
- (12) Zhao, B.; Brittain, W. J. *Prog. Polym. Sci.* **2000**, *25*, 677–710.
- (13) Ballauff, M.; Borisov, O. *Curr. Opin. Colloid Interface Sci.* **2006**, *11*, 316–323.
- (14) Guo, X.; Ballauff, M. *Langmuir* **2000**, *16*, 8719–8726.
- (15) Minko, S. *Polym. Rev.* **2006**, *46*, 397–420.
- (16) Jimenez, J.; de Joannis, J.; Bitsanis, I.; Rajagopalan, R. *Macromolecules* **2000**, *33*, 7157–7164.
- (17) Papastavrou, G.; Kirwan, L. J.; Borkovec, M. *Langmuir* **2006**, *22*, 10880–10884.
- (18) Hugel, T.; Seitz, M. *Macromol. Rapid Commun.* **2001**, *22*, 989–1016.
- (19) Giannotti, M. I.; Vancso, G. J. *ChemPhysChem* **2007**, *8*, 2290–2307.
- (20) Janshoff, A.; Neitzert, M.; Oberdorfer, Y.; Fuchs, H. *Angew. Chem., Int. Ed.* **2000**, *39*, 3213–3237.
- (21) Minko, S.; Roiter, Y. *Curr. Opin. Colloid Interface Sci.* **2005**, *10*, 9–15.
- (22) Sonnenberg, L.; Parvole, J.; Borisov, O.; Billon, L.; Gaub, H. E.; Seitz, M. *Macromolecules* **2006**, *39*, 281–288.
- (23) Sonnenberg, L.; Parvole, J.; Kühner, F.; Billon, L.; Gaub, H. E. *Langmuir* **2007**, *23*, 6660–6666.
- (24) Chatellier, X.; Senden, T. J.; Joanny, J. F.; di Meglio, J. M. *Europhys. Lett.* **1998**, *41*, 303–308.
- (25) Hugel, T.; Grosholz, M.; Clausen-Schaumann, H.; Pfau, A.; Gaub, H. E.; Seitz, M. *Macromolecules* **2001**, *34*, 1039–1047.
- (26) Conti, M.; Bustanji, Y.; Falini, G.; Ferruti, P.; Stefoni, S.; Samori, B. *ChemPhysChem* **2001**, *2*, 610–613.
- (27) Cui, S. X.; Liu, C. J.; Wang, Z. Q.; Zhang, X. *Macromolecules* **2004**, *37*, 946–953.
- (28) Friedsam, C.; Gaub, H. E.; Netz, R. R. *Europhys. Lett.* **2005**, *72*, 844–850.
- (29) Hanke, F.; Livadaru, L.; Kreuzer, H. J. *Europhys. Lett.* **2005**, *69*, 242–248.
- (30) Sonnenberg, L.; Luo, Y. F.; Schlaad, H.; Seitz, M.; Colfen, H.; Gaub, H. E. *J. Am. Chem. Soc.* **2007**, *129*, 15364–15371.
- (31) Geisler, M.; Pirzer, T.; Ackerschott, C.; Lud, S.; Garrido, J.; Scheibel, T.; Hugel, T. *Langmuir* **2008**, *24*, 1350–1355.
- (32) Laruelle, G.; Francois, J.; Billon, L. *Macromol. Rapid Commun.* **2004**, *25*, 1839–1844.
- (33) Parvole, J.; Montfort, J. P.; Reiter, G.; Borisov, O.; Billon, L. *Polymer* **2006**, *47*, 972–981.
- (34) Al-Maawali, S.; Bemis, J. E.; Akhremitchev, B. B.; Leecharoen, R.; Janesko, B. G.; Walker, G. C. *J. Phys. Chem. B* **2001**, *105*, 3965–3971.
- (35) Goodman, D.; Kizhakkedathu, J. N.; Brooks, D. E. *Langmuir* **2004**, *20*, 3297–3303.
- (36) Kühner, F.; Erdmann, M.; Sonnenberg, L.; Serr, A.; Morfill, J.; Gaub, H. E. *Langmuir* **2006**, *22*, 11180–11186.
- (37) Serr, A.; Netz, R. R. *Europhys. Lett.* **2006**, *73*, 292–298.
- (38) Haupt, B. J.; Senden, T. J.; Seivick, E. M. *Langmuir* **2002**, *18*, 2174–2182.
- (39) Scherer, A.; Zhou, C. Q.; Michaelis, J.; Brauchle, C.; Zumbusch, A. *Macromolecules* **2005**, *38*, 9821–9825.
- (40) Senden, T. J.; di Meglio, J. M.; Auroy, P. *Eur. Phys. J. B* **1998**, *3*, 211–216.
- (41) Friedsam, C.; Becares, A. D.; Jonas, U.; Seitz, M.; Gaub, H. E. *New J. Phys.* **2004**, *6*, 9.
- (42) Seitz, M.; Friedsam, C.; Jostl, W.; Hugel, T.; Gaub, H. E. *ChemPhysChem* **2003**, *4*, 986–990.
- (43) Kühner, F.; Erdmann, M.; Gaub, H. E. *Phys. Rev. Lett.* **2006**, *97*, 218301.
- (44) Gennes, P.-G. d. *Scaling Concepts in Polymer Physics*; Cornell University Press: Ithaca, NY, 1979.

MA702600Y